MACROSCOPIC CHARACTERISTICS OF LANE-CHANGING TRAFFIC

WEN-LONG JIN[1]

Department of Civil and Environmental Engineering
California Institute for Telecommunications and Information Technology
Institute of Transportation Studies
4038 Anteater Instruction and Research Bldg
University of California
Irvine, CA 92697-3600
Tel: 949-824-1672
Fax: 949-824-8385
Email: wjin@uci.edu

Word Count: 5000+250×10=7500

November 15, 2009

SUBMITTED TO 2010 TRB ANNUAL MEETING

[1]Author for correspondence

ABSTRACT

On a multi-lane roadway, systematic lane-changes can seriously disrupt traffic flow and cause capacity reductions. Therefore it is important to understand the characteristics of lane-changing traffic flow. In our previous study, a new variable, lane-changing intensity, was theoretically derived by doubling the contribution to the total density of a lane-changing vehicle during its lane-changing period, and a intensity-density relation was incorporated into the fundamental diagram to capture such bottleneck effects at the aggregate level. In this study, we propose a new interpretation of lane-changing intensity by following Edie's definition of traffic density. We then present our detailed studies of macroscopic characteristics of lane-changing traffic with 75 minutes of vehicle trajectories collected for a freeway section on interstate 80 by the NGSim project. Here we are able to exclude about 10% misindentified lane-changes. For different time intervals, cell sizes, and locations, we further verify the well-definedness of the lane-changing intensity variable and intensity-density relation. Future directions are discussed in the conclusion section.

Keywords: Lane-changing intensity, intensity-density relationship, modified fundamental diagram, NGSim project, lane-changing threshold

List of Tables

List of Figures

1 Introduction

In a road network, lane-changing areas, where one or more streams of vehicles systematically change their lanes, could constitute significant bottlenecks [1] and cause accidents [e.g. 2]. Therefore it is important to understand characteristics of lane-changing traffic flow and the behaviors of lane-changing vehicles.

In the literature, there have been many studies of vehicles' behaviors related to lane-changing motive, time, location, and manuver at the microscopic level [3, 4, 5, 6]. On the other hand, many studies have been carried out to understand various characteristics of lane-changing traffic at the macroscopic level: the exchange of flows between lanes [7, 8, 9, 10], density oscillation and instability issues [11, 12], and the degree of First-In-First-Out violation among vehicles [13]. Since the publication of Highway Capacity Manual in 1950, there have been many studies on the level of service of weaving areas, which are special lane-changing areas [e.g. 14]. In [15], a hybrid micro-/macro-scopic model was proposed to study lane-changing traffic dynamics. In [16], a new macroscopic model was proposed to capture lateral interactions among vehicles in the framework of fundamental diagram [17]. In addition to traffic density, $\rho(x,t)$, travel speed, $v(x,t)$, and flow-rate, $q(x,t)$, a new variable of lane-changing intensity, $\epsilon(x,t)$, was introduced to account for the level of lane-changing activities at location x and time t. Roughly, ϵ can be considered as the ratio of vehicles' lane-changing time to their total travel time in a road section in a space-time domain. Furthermore, an intensity-density relation was hypothesized and incorporated into the fundamental diagram to study the impacts of lane-changing traffic on overall traffic flow. Some results with observed data were shown to demonstrate that such an intensity-density relationship is yet another fundamental relationship for lane-changing traffic.

In this study, we propose a new interpretation of lane-changing intensity in [16] by extending Edie's definition of traffic density. We then present our detailed studies of macroscopic characteristics of lane-changing traffic with 75 minutes of vehicle trajectories collected for a freeway section on interstate 80 by the NGSim project. In particular, we will examine the consistency of the data sets very carefully to exclude misidentified lane-changes caused by limitations in video transcription. Then for different lane-changing thresholds, time intervals, cell sizes, and locations, we further verify the well-definedness of the lane-changing intensity variable and intensity-density relation.

The rest of the paper is organized as follows. In Section 2, we introduce a macroscopic theory of lane-changing traffic and discuss lane-changing effect in a uniform traffic flow. In Section 3, we describe four data sets for studying real lane-changing traffic. In Section 4, we present algorithms for computing aggregate lane-changing traffic characteristics. In Section 5, we study the macroscopic lane-changing intensity and the corresponding fundamental diagram for various scenarios. In Section 6, we conclude our study with some discussions.

2 A macroscopic lane-changing theory

2.1 Review of a macroscopic lane-changing theory

In [16], a macroscopic lane-changing theory was proposed based on the observation that, in congested traffic, a lane-changing vehicle impacts traffic flow on both its previous lane and its target lane. In this theory, the movement of a lane-changing is considered in a three-dimensional (x, y, t) space: longitudinal direction x, lateral direction y, and time t. In particular, a lane-change can be described by the lane-changing period of $\Delta t \equiv t_{LC}$ and two displacements Δx and Δy in the x and y directions, respectively. Furthermore the lateral displacement threshold of the lane-changing vehicle, or simply lane-changing threshold, Δy, should be at least the width of the vehicle w. In summary, a lane-change can be described by the following variables:

- Previous lane and target lane;
- Lane-changing location and time in the (x, y, t) space, (x_{LC}, y_{LC}, t_{LC});
- Lane-changing distances and duration in the (x, y, t) space, $(\Delta x, \Delta y, \Delta t)$;
- Lane-changing angle, θ, where $\tan\theta = \frac{\Delta y}{\Delta x}$;
- Longitudinal speed, $v = \frac{\Delta x}{\Delta t}$.

Here the variables follow the following relationship

$$t_{LC} \equiv \Delta t = \frac{\Delta y}{v \tan\theta}. \tag{1}$$

At the aggregate level, in a space-time domain, $[x_a, x_b] \times [t_a, t_b]$, lane-changing traffic can be described by the following quantities:

- The number of lane-changes, N_{LC};
- Total lane-changing time, $N_{LC} t_{LC}$;
- Lane-changing traffic density, ρ_{LC};
- Lane-changing traffic flow-rate, q_{LC}.

Then in [16], based on the argument that the contribution of lane-changing vehicles should be doubled during their lane-changing periods, the effective density of total traffic was defined for a lane-changing area with a width of $L = x_b - x_a$ and time period with a duration of $T = t_b - t_a$

$$\bar{\rho} = \frac{\rho LT + N_{LC} t_{LC}}{LT} = \rho + \frac{N_{LC} t_{LC}}{LT} = (1 + \epsilon)\rho, \tag{2}$$

where a new lane-changing intensity variable, ϵ, was given by

$$\epsilon(x,t) \;=\; \frac{N_{LC}t_{LC}}{\rho LT} = \frac{N_{LC}t_{LC}}{NT}. \tag{3}$$

As expected, lane-changing intensity is determined by the number of lane-changes, the lane-changing duration, and traffic density in the lane-changing area. Thus for lane-changing traffic we have four aggregate variables: traffic density $\rho(x,t)$, travel speed $v(x,t)$, flow-rate $q(x,t)$, and lane-changing intensity $\epsilon(x,t)$. In the literature the first three variables have been well defined and can be measured; in this study the fourth is defined in **Equation** 3 and will be measured for real traffic. Furthermore, we will try to calibrate the relationship between lane-changing intensity and traffic density under various conditions. That is, empirical observations support the following intensity-density relationship

$$\epsilon \;=\; E(x,\rho). \tag{4}$$

Furthermore, a modified speed-density relationship was introduced for a lane-changing area $v(x,t) = V((1+\epsilon(x,t))\rho(x,t))$, where $V(\cdot)$ is the speed-density relationship without lane-changing effect. Therefore, with higher lane-changing intensity, the same traffic density would lead to higher effective total density and lower average speed. Then, the fundamental diagram with lane-changing effect is

$$q \;=\; \rho V((1+\epsilon)\rho). \tag{5}$$

Based on the assumption that **Equation** 5 is the true fundamental diagram for lane-changing traffic, the fundamental diagram without lane-changing can be obtained as

$$q \;=\; Q(\bar{\rho}) = \bar{\rho}V(\bar{\rho}) = (1+\epsilon)\rho V((1+\epsilon)\rho). \tag{6}$$

By comparing **Equation** 6 and **Equation** 5, we will be able to understand the impact of lane-changing traffic. In [16], the LWR model [18, 19] was extended to incorporate lane-changing effect

$$\frac{\partial \rho}{\partial t} + \frac{\partial \rho V((1+\epsilon)\rho)}{\partial x} \;=\; 0. \tag{7}$$

With **Equation** 4, we can have the following conservation law

$$\frac{\partial \rho}{\partial t} + \frac{\partial \rho V((1+E(x,\rho))\rho)}{\partial x} \;=\; 0.$$

The kinematic wave solutions of **Equation** 7 were studied in [16].

2.2 A new interpretation of lane-changing intensity variable

Edie's definition of the average traffic density in a space-time domain A [20, 21] is given by

$$\rho(A) = \frac{\sum t_i}{|A|},$$

where t_i is the time for vehicle i in the domain, and $|A|$ the area of the domain. Following Edie's definition, we can define the effective density by

$$\bar{\rho}(A) = \frac{\sum t_i + t_{i,LC}}{|A|}, \tag{8}$$

where $t_{i,LC}$ is the lane-changing time of vehicle i in the domain. Therefore, lane-changing intensity in the domain A can be defined by

$$\epsilon(A) = \frac{\sum t_{i,LC}}{\sum t_i}. \tag{9}$$

Therefore, lane-changing intensity can be considered the ratio of the total lane-changing time to the total time that vehicles spend in a space-time domain. Here **Equation** 9 can be considered as an extension of **Equation** 3, where the domain is $[x_a, x_b] \times [t_a, t_b]$. With this interpretation, the theories developed in [16] are valid for all space-time domains.

3 Data sets and pre-processing

In this study, we carefully analyze lane-changing traffic on a six-lane freeway section on interstate 80 in Emeryville (San Francisco), California, as shown in Figure 1. Here lane 1 is a car-pool lane, and there is an on-ramp from Powell Street and an off-ramp to Ashby Ave. The road section is covered by seven cameras, numbered 1 to 7 from south to north (also traffic direction), and the original videos are transcribed into vehicle trajectories by FHWA's NGSIM project [22]. Four data sets are available to the public [23, 24, 25, 26]: data set 1 with vehicle trajectories of every fifteenth second on December 3, 2003 between 2:35pm and 3:05pm, and data sets 2 to 4 with vehicle trajectories of every tenth second on April 13, 2005 between 4pm and 4:15pm, between 5pm and 5:15pm, and between 5:15pm and 5:30pm, respectively. Here vehicles' trajectories are transcribed with different lengths between the first and the other three data sets: vehicles' trajectories extend to the downstream Ashby Ave off-ramp in the first data set, but not in the other three.

A vehicle at each time instant or frame has 16 describing quantities in the first data set and 18 in the other three data sets. The same 16 quantities are the ID of a vehicle (Vehicle ID), total number of video frames that the vehicle presents (Total Frames), the ID of a video frame (Frame ID), the elapsed time since January 1, 1970 (Global Time), lateral distance of the front center of the vehicle from the left-most edge of the section (Local X),

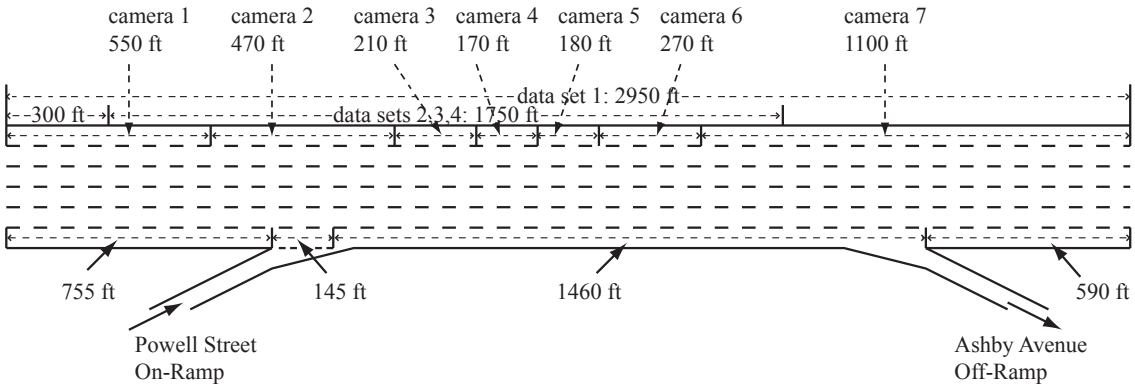

Figure 1: The I-80 study area

longitudinal distance of the front center of the vehicle from the entry edge of the section (Local Y), the X coordinate of the front center of the vehicle based on CA State Plane III in NAD83 (Global X), the Y coordinate of the front center of the vehicle based on CA State Plane III in NAD83 (Global Y), the length of the vehicle (Vehicle Length), the width of the vehicle (Vehicle Width), the class of vehicle (Vehicle Class: 1 for motorcycles, 2 for autos, and 3 for trucks), instantaneous velocity of the vehicle (Vehicle Velocity), instantaneous acceleration of the vehicle (Vehicle Acceleration), the current lane position of the vehicle (Lane Identification: 1 is the left-most lane, 6 is the right-most lane, 7 is the on-ramp from Powell Street, and 8 is the off-ramp to Ashby Avenue), vehicle ID of the leading vehicle in the same lane (Preceding Vehicle), and vehicle ID of the following vehicle in the same lane (Following Vehicle). In data sets 2 to 4, two additional quantities are used: the spacing between the vehicle and its leader (Spacing), and the headway between the vehicle and its leader (Headway). Here the unit of length is feet, and the unit of time is second.

We determine the coverage of cameras shown in Figure 1 by playing the videos for data set 2 frame by frame. We find the location of a vehicle when its front reaches the end of the region covered by a camera. From the trajectory and video of vehicle 1, the ends of the regions covered by cameras 1 through 6 in global y (local y) are 2133295 ft (250 ft), 2133762 ft (720 ft), 2133931 ft (910 ft), 2134104 ft (1080 ft), 2134294 ft (1260 ft), and 2134560 ft (1530 ft), respectively; the on-ramp ends at 2133645 ft (605 ft). From the trajectory and video of vehicle 100, the ends of the regions covered by cameras 1 through 6 in global y (local y) are 2133303 ft (235 ft), 2133768 ft (700 ft), 2133938 ft (871 ft), 2134112 ft (1048 ft), 2134296 ft (1235 ft), 2134560 ft (1502 ft), respectively; the on-ramp ends at 2133655 ft (586 ft). We can see that the errors in the camera coverage are about 10 ft in global y and 30 ft in local y. From the analysis, the longitudinal distances are subject to measuring errors in the order of 10 ft. Note that, the cameras are mounted on high buildings to the east of the road section, and a vehicle's shadow is on its east side. Such a set-up can cause

misidentification of vehicles, and errors occur in the lateral direction.

3.1 Consistency of data

In the following, we first check the consistency of these data sets. Here we use data set 2 as an example: 1) the frame ID's of each vehicle in column 2 are different; 2) the total number of frames in column 3 is correct; 3) each vehicle has unique length in column 9, width in column 10, and class in column 11. We also verify that the longitudinal distance from the entry edge of the study section in column 6 is not decreasing with respect to time for each vehicle, since vehicles are not allowed to travel backward.

We then verify that the frame ID in column 2 is consistent with the global time in column 4. The first frame is at 3:58:55pm on April 13, 2005 of California local time. Since Californias time zone is UTC-7 (Coordinated Universal Time) on this day, the first frame corresponds to 10:58:55pm on April 13, 2005 of Greenwich Mean Time (GMT). The elapsed time for the first frame since January 1, 1970 equals $9 \cdot 366 + 26 \cdot 365 + (31 + 28 + 31 + 12) = 12886$ days plus 23 hours minus 65 seconds. Thus the first frame's global time is 1113433135000 ms. For example, the first frame that vehicle 1 appears is 12, and the global time is 1113433135000+1100=113433136100 ms. Therefore, the data in columns 2 and 4 are consistent.

For data set 1, we can obtain a linear relationship between local longitudinal coordinates (local y in column 5) and global longitudinal coordinates (global y in column 7) as

$$globaly \approx 2132777.951 + 0.9894 localy$$

with R-square of 0.99998. For data sets 2 to 4, we have

$$globaly \approx 2133073.377 + 0.9911 localy$$

with R-square of 0.99995. Thus in the local longitudinal coordinate, the upstream edge in data sets 2 to 4 is at about 298 ft in data set 1. However, we cannot find simple linear relationship between local x and global x. This could be caused by the specific coordinate system used and the special geometric shape of the road section. It also could be caused by measuring errors. Here we will use local lateral coordinate for our study of lane-changing traffic. Note that, in the data sets, local x and y correspond to y and x in our formulations, respectively.

3.2 Identification of lane-changes

In this subsection, we discuss how to extract characteristics of individual lane changes with data set 2, for which we use processed video files to verify our results. For the whole data set, we first identify all vehicles that occupied two or more lanes from their lane information and distinguish their classes. We find that, from the given lane information, totally 670

vehicles, including one motorcycle, 25 trucks, and 644 autos, made lane-changes. For each lane-change, we find its vehicle ID, time, longitudinal location, lateral location, previous lane, and target lane. For all lane-changing vehicles, we identify its vehicle ID, vehicle class, total number of lane-changes, initial lateral location, initial longitudinal location, initial lane, and initial time in the trajectory data set. For data set 2, totally 1043 lane-changes are found: 429 vehicles made one lane-change, 158 vehicles made two, 54 vehicles made three, 16 made four, 6 made five, 7 made six.

We find that some lane-changes are false due to mistakenly identify a vehicle's shadow as itself. Such a misidentification usually occurs for vehicles with wide shadows and when they are at the boundaries of cameras. For example, vehicle 1456, a truck, is misidentified from 448s to 448.5s when entering the covering area of camera 3. Since the shadow is to the west of a vehicle, a misidentification results in a lane number which is one greater. Therefore, we remove the two lane-changes of the same vehicle, if (1) they are within 4 s from each other, (2) the previous lane of the earlier one is the same as the target lane of the later one, and (3) the target lane of the later one is smaller than the previous lane. That is, if a vehicle is swerving to the east and then back in a very short time, it is probably caused by misidentification. For the 1043 lane-changes, we remove 104 such false lane-changes, which are randomly verified with video data. For the 104 false lane-changes, motorcycles, autos, and trucks made 2, 82, and 20 of them, respectively; for the remaining 939 lane-changes, motorcycles, autos, and trucks made 0, 912, and 27 of them, respectively.

Further, we exclude 190 lane-changes from lane 7 to lane 6, since vehicles do not really change lanes when merging, but only to continue on a new lane. We also exclude 22 lane-changes of mainline vehicles to and from lane 7. In the final 727 lane-changes, 133 are made by 86 on-ramp vehicles, and 594 are made by 451 mainline vehicles. Averagely, each mainline lane-changing vehicle makes 1.32 lane-changes, and each on-ramp lane-changing vehicle makes 1.55 lane-changes. In the final 727 lane-changes, 23 are made by 16 trucks, and 704 are made by 521 autos. Averagely, each truck makes 1.44 lane-changes, and each auto makes 1.35 lane-changes.

For each lane-change, we extract its trajectory as follows. Assume that lane-change occurs at y_{lc}, we set a threshold of $[y_{lc} - \Delta y/2, y_{lc} + \Delta y/2]$. In our study, we choose Δy as the width of a vehicle w (between 4.8 ft and 8.5 ft for vehicles in data set 2), or $3/2w$. Then we find the starting and ending times, x, and y of a lane-change. We also assume that the lane-changing time on each side cannot be bigger than 25 s. For data set 2, we find that zero lane-changes with lane-changing times greater than 40 s are false, but exclude four lane-changes that finish within 10 ft in the longitudinal direction. The final number of valid lane-changes is 723. For data set 2, the greatest and smallest angles are 21.38 and 0.10 degrees, respectively; the greatest and smallest lane-changing times are 39.6 and 0.4 s, respectively; the greatest and smallest speeds are 46.95 and 9.00 mph, respectively.

4 Computation of macroscopic lane-changing characteristics

We consider the lane-changing traffic in the weaving section downstream to the on-ramp and upstream to the off-ramp in a space-time domain of $[x_a, x_b] \times [t_a, t_b]$. Ideally, all vehicles in $[x_a, x_b] \times [t_a, t_b]$ should be detected.

4.1 Computation of density, speed, and flow-rate

In Figure 2, the trajectories on different lanes are shown in the domain of $[650, 1550] \times [390, 453]$ in data set 2. Broken trajectories are caused by lane-changes.

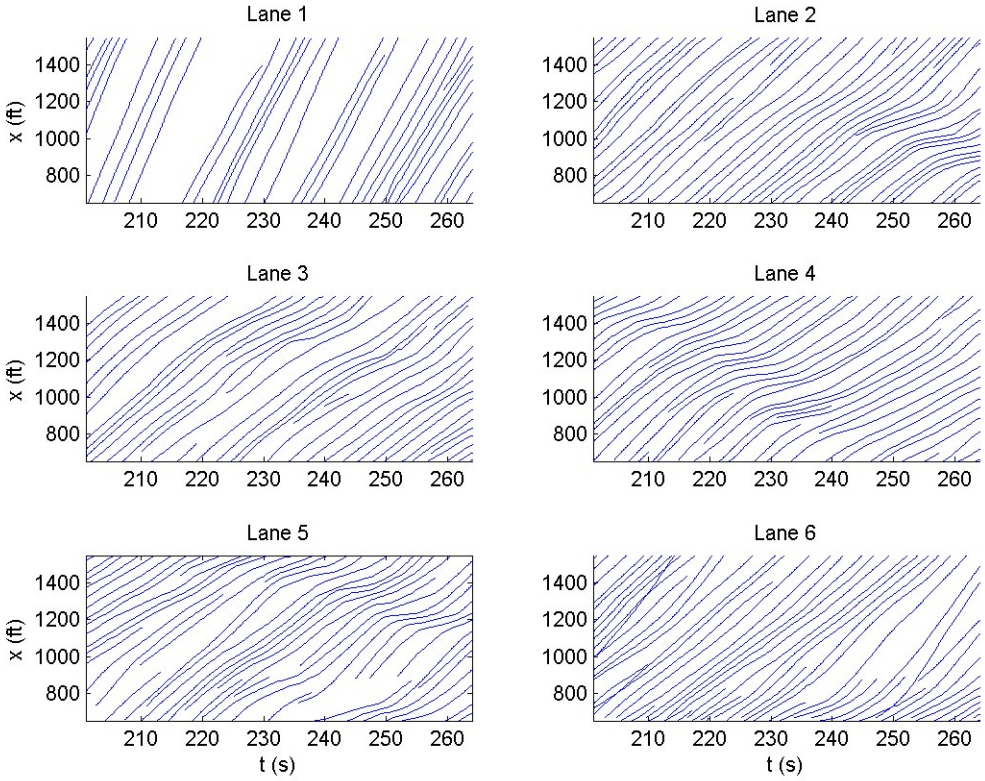

Figure 2: Vehicle trajectories in $[650, 1550] \times [390, 453]$ in data set 2

Assuming that N is the number of vehicles in the domain of $[x_a, x_b] \times [t_a, t_b]$. At time t_j, where $j = 1, \cdots, J$, $t_j \in [t_a, t_b]$, and $t_{j+1} - t_j = \Delta t_j = \frac{t_b - t_a}{J}$, we can find the number of vehicles in the region $[x_a, x_b]$, $N([x_a, x_b]; t_j)$. As shown in Figure 3 for the domain of

$[650, 1550] \times [201, 264]$, the dots on the horizontal line show all vehicles in the region at $t_j = 232$ s. Then the average density is

$$\rho([x_a, x_b] \times [t_a, t_b]) \quad = \quad \frac{\sum_{j=1}^{J} N([x_a, x_b]; t_j)}{J(x_b - x_a)}. \tag{10}$$

If we denote the total time that all vehicles spend in the domain $[x_a, x_b] \times [t_a, t_b]$ by $N \cdot T$, then

$$\begin{aligned} N \cdot T \quad &\approx \quad \sum_j N([x_a, x_b]; t_j)\Delta t_j = J\rho([x_a, x_b] \times [t_a, t_b])(x_b - x_a)\frac{t_b - t_a}{J} \\ &= \quad \rho([x_a, x_b] \times [t_a, t_b])(x_b - x_a)(t_b - t_a). \end{aligned}$$

That is, $N \cdot T \approx \rho LT$, if $L = x_b - x_a$ and $T = t_b - t_a$. Thus density is the ratio of vehicles' total travel time to the size of the domain. Therefore, the formula in **Equation** 10 is an approximation to Edie's definition of traffic density in a space-time domain [20, 21], and the approximation error decreases when we increase the number of samples, J.

Similarly, we can sample the trajectories of vehicles in the domain $[x_a, x_b] \times [t_a, t_b]$ at location x_i, where $x_i \in [x_a, x_b]$ and $x_{i+1} - x_i = \Delta x_i = \frac{x_b - x_a}{I}$, we can compute the average flow-rate by

$$q([x_a, x_b] \times [t_a, t_b]) \quad = \quad \frac{\sum_i N(x_i; [t_a, t_b])}{I(t_b - t_a)}. \tag{11}$$

Thus flow-rate can be considered as the ratio of vehicles' total travel distance to the size of the domain, and **Equation** 11 is an approximation to Edie's definition of flow-rate in a space-time domain [20, 21]. As shown in Figure 3, the dots on the vertical line show all vehicles in the time interval at $x_i = 1100$ ft. We can then compute the average speed as

$$v_1([x_a, x_b] \times [t_a, t_b]) \quad = \quad q([x_a, x_b] \times [t_a, t_b])/\rho([x_a, x_b] \times [t_a, t_b]).$$

For vehicle n in the domain, we can find its speed as $v_n = \Delta x_n / \Delta t_n$. Then, the space-mean speed is

$$v_2([x_a, x_b] \times [t_a, t_b]) \quad = \quad \frac{N}{\sum_{n=1}^{N} 1/v_n},$$

and the time-mean speed is

$$v_3([x_a, x_b] \times [t_a, t_b]) \quad = \quad \frac{\sum_{n=1}^{N} v_n}{N}.$$

In **Table** 1, we demonstrate the mean values and standard deviations of density, flow-rate, and speed for data set 2 for different time intervals. From the table, we can see that ρ and q are computed more accurately than v_2 and v_3. Thus, hereafter we will use v_1. Generally, $v_2 < v_1 < v_3$. But v_1 is very close to the space-mean speed v_2.

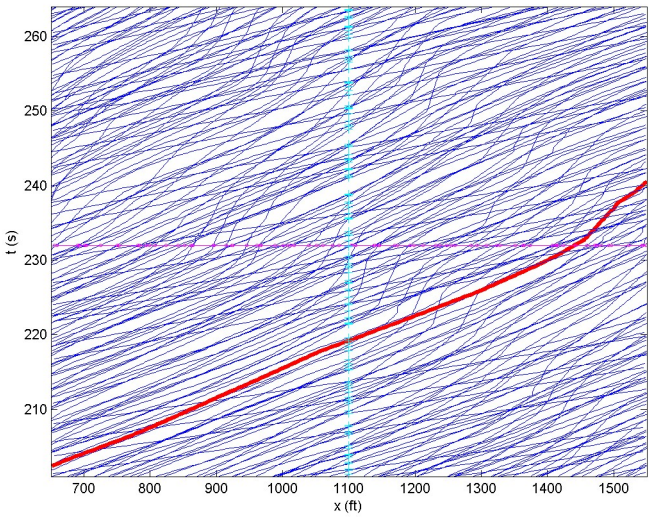

Figure 3: An illustration of the computation of density, flow-rate, and speed

$[t_a, t_b]$	75-	138-	201-	264-	327-	390-	453-	516-	579-	642-	705-	768-	831-
ρ	4.33e2	4.15e2	4.44e2	3.83e2	4.16e2	4.42e2	4.81e2	4.64e2	5.14e2	5.18e2	4.76e2	5.54e2	4.74e2
std	4.68e1	1.87e1	2.00e1	3.84e1	9.38e0	2.02e1	5.14e1	3.79e1	5.80e1	4.57e1	2.09e1	3.53e1	3.03e1
q	8.16e3	8.52e3	8.02e3	8.43e3	9.10e3	8.00e3	7.48e3	8.20e3	7.82e3	7.87e3	8.53e3	6.60e3	8.39e3
std	4.82e2	7.64e1	1.55e2	1.75e2	1.43e2	1.86e2	2.99e2	2.97e2	5.59e2	4.01e2	2.27e2	1.45e2	1.97e2
v_1	18.83	20.53	18.06	22.04	21.90	18.12	15.54	17.66	15.22	15.18	17.92	11.92	17.71
v_2	18.61	20.34	17.18	22.01	21.44	16.84	13.59	17.24	13.59	14.79	17.16	11.05	17.26
$1/v_2$	5.4e-2	4.9e-2	5.8e-2	4.5e-2	4.7e-2	5.9e-2	7.4e-2	5.8e-2	7.4e-2	6.8e-2	5.8e-2	9.1e-2	5.8e-2
std	1.6e-2	1.1e-2	1.9e-2	1.2e-2	1.3e-2	1.8e-2	3.8e-2	1.9e-2	3.9e-2	2.3e-2	1.8e-2	3.9e-2	1.5e-2
v_3	20.47	22.29	20.09	23.89	23.64	19.48	18.53	20.44	17.28	17.14	19.43	14.81	18.99
std	7.03	9.14	10.07	7.51	8.32	9.87	12.37	10.82	10.14	7.98	8.25	10.49	7.21

Table 1: Computation of density, flow-rate, and speed

4.2 Aggregate characteristics of lane-changes

In Figure 4, we show the trajectories of 30 vehicles in data set 2 that made lane-changes in the domain of $[650, 1550] \times [201, 264]$. The horizontal line shows all lane-changing vehicles in the region at $t = 232$, and with a formula similar as **Equation** 10 we can find the lane-changing density ρ_{LC} in the domain. The vertical line shows all lane-changing vehicles in the time interval at $x = 1100$, and with a formula similar as **Equation** 11 we can find the lane-changing flow-rate q_{LC} in the domain. In the figure, the red line is the trajectory for vehicle 576, and the thicker line segment is the trajectory when it is making a lane-change. In the model of **Equation** 3, when vehicle 576 is on the thicker line segment, its contribution to the density should be doubled. Furthermore, we can find the total number of lane-changes N_{LC} in the domain, the average lane-changing time t_{LC}, and the total lane-changing time $n_{LC}t_{LC}$. We can also find the average number of lane-changes by each lane-changing vehicle,

$[t_a, t_b]$	75-	138-	201-	264-	327-	390-	453-	516-	579-	642-	705-	768-	831-
ρ_{LC}	77.37	59.58	91.30	49.50	50.23	57.66	50.97	57.29	59.22	55.73	74.43	63.98	61.60
std	22.29	21.07	29.69	15.25	5.00	19.96	11.73	5.51	10.59	7.68	17.86	10.39	17.71
q_{LC}	1.34e3	1.14e3	1.48e3	1.02e3	9.93e2	9.76e2	6.64e2	9.59e2	7.59e2	6.99e2	1.14e3	6.02e2	9.60e2
std	9.21e1	1.31e2	1.51e2	1.37e2	7.69e1	7.62e1	7.56e1	6.90e1	8.22e1	1.14e2	2.60e2	9.58e1	1.12e2
θ	5.22	4.52	5.80	3.73	4.52	4.63	4.57	5.66	6.66	5.84	5.66	6.67	5.93
std	2.80	2.03	3.18	1.80	1.93	1.77	2.38	2.98	4.04	4.16	2.64	2.74	2.56
t_{LC}	3.82	3.39	3.56	4.25	3.69	3.35	6.08	2.68	3.00	5.62	4.15	4.36	3.14
std	2.28	1.99	3.33	3.10	3.68	2.03	8.83	1.32	1.57	4.59	4.39	4.86	1.54

Table 2: Computation of aggregate lane-changing characteristics

$\alpha = \frac{N_{LC}}{\rho_{LC} L}$.

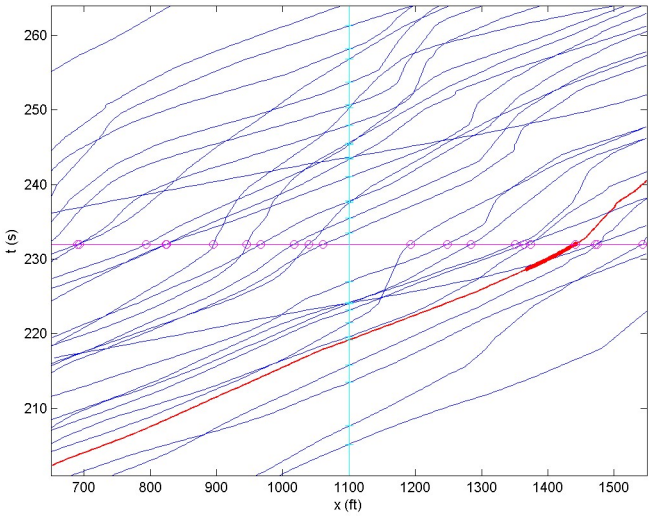

Figure 4: Aggregate properties of lane-changes

If a lane-change occurs in the space-time domain $[x_a, x_b] \times [t_i, t_i + T]$, we then count it as one lane-change in the domain. Thus we can obtain the number of lane-changes, N_{LC}. For all the lane-changes, we can find the average angles, θ, the average number of lane-changes for each vehicle in the domain, the total time for lane-changes $N_{LC} t_{LC}$, and the average lane-changing time t_{LC}. In **Table** 2, we show the mean values and standard deviations of ρ_{LC}, q_{LC}, θ, and t_{LC} for data set 2. We can see that the standard deviation of t_{LC} could be greater than its mean. For all these values, q_{LC} is the best estimated.

5 Calibration of the relationship between lane-changing intensity and traffic density

In [16], the impacts of lane-changing thresholds were discussed. In the following, we compute lane-changing intensity ϵ based on **Equation** 3 and calibrate $\epsilon = E(x, \rho)$, the relationship between lane-changing intensity and traffic density, for different time-steps, cell sizes, and locations. Here we also discuss the impacts of lane-changing traffic on capacity with **Equation** 6 and **Equation** 5.

5.1 Different time-steps

In this subsection, we have the same road section as in the preceding subsection and set $\Delta y = w$. First, we set T=12, 35, 48, 56 s for four data sets, respectively. From Figure 5, we find a linear relationship between density and lane-changing angle

$$\theta = -0.5233 + 0.0122\rho,$$

with R-square 0.8746. We can also find the following relationship between density and ϵ

$$\epsilon = 0.2251e^{-0.0046\rho},$$

with R-square 0.6903. From data we have that $q = \rho V(\rho)$ has a capacity of 15316 mph when $\rho = 251$ vpm, and $q = \rho V((1 + \epsilon)\rho)$ has a capacity of 13309 mph when $\rho = 232$ vpm. The lane-changes cause a capacity reduction of 13.10%.

Then we set $T = 10$ s for all data sets, we have the following results. We find a linear relationship between density and lane-changing angle

$$\theta = -0.5953 + 0.0126\rho,$$

with R-square 0.6421. We can also find the following relationship between density and ϵ

$$\epsilon = 0.2039e^{-0.0044\rho},$$

with R-square 0.5977. We can see that $q = \rho V(\rho)$ has a capacity of 14893 mph when $\rho = 253$ vpm, and $q = \rho V((1+\epsilon)\rho)$ has a capacity of 13520 mph when $\rho = 232$ vpm. The lane-changes cause a capacity reduction of 9.22%.

With shorter time intervals T, we can have more domains $[x_a, x_b] \times [t_i, t_i + T]$. We can see that different time intervals can yield different results, but both the aggregate lane-changing characteristics and fundamental diagrams are of the same magnitude.

5.2 Different cell sizes

In this subsection, we consider different road sections downstream to the on-ramp in Figure 1.

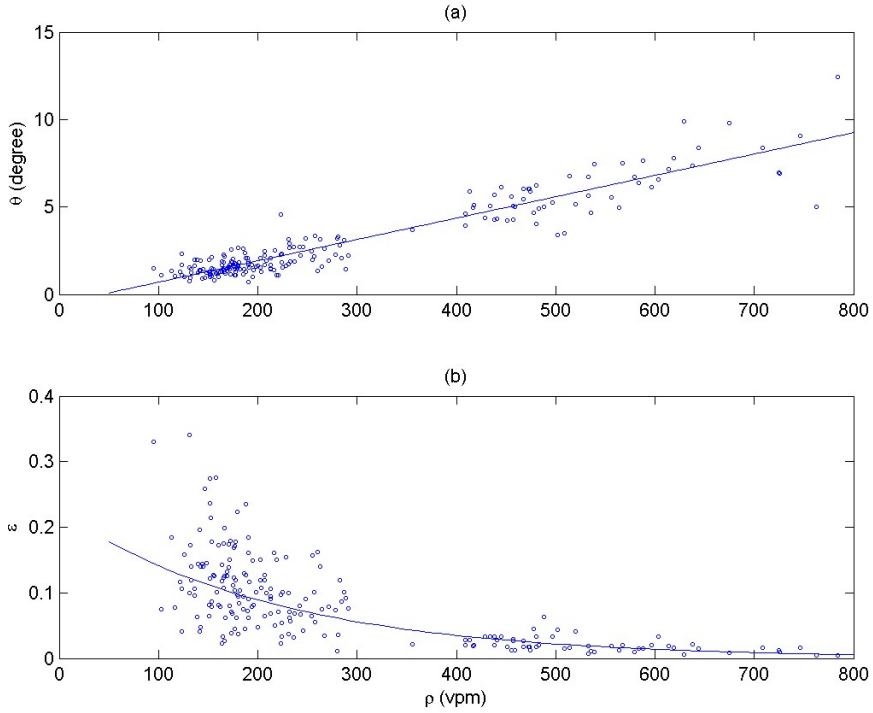

Figure 5: Characteristics of lane-changes at different densities with T=12, 35, 48, 56 s

First, we consider a road section $[950, 1400]$. From Figure 7, we find a linear relationship between density and lane-changing angle

$$\theta = -0.2633 + 0.0118\rho,$$

with R-square 0.8702. We can also find the following relationship between density and ϵ

$$\epsilon = 0.2116e^{-0.0042\rho},$$

with R-square 0.7630. From data we have that $q = \rho V(\rho)$ has a capacity of 13231 mph when $\rho = 214$ vpm, and $q = \rho V((1+\epsilon)\rho)$ has a capacity of 12073 mph when $\rho = 196$ vpm. The lane-changes cause a capacity reduction of 8.76%.

We consider a road section $[1400, 1850]$. From Figure 9, we find a linear relationship between density and lane-changing angle

$$\theta = -0.5967 + 0.0119\rho,$$

with R-square 0.8819. We can also find the following relationship between density and ϵ

$$\epsilon = 0.3074e^{-0.0059\rho},$$

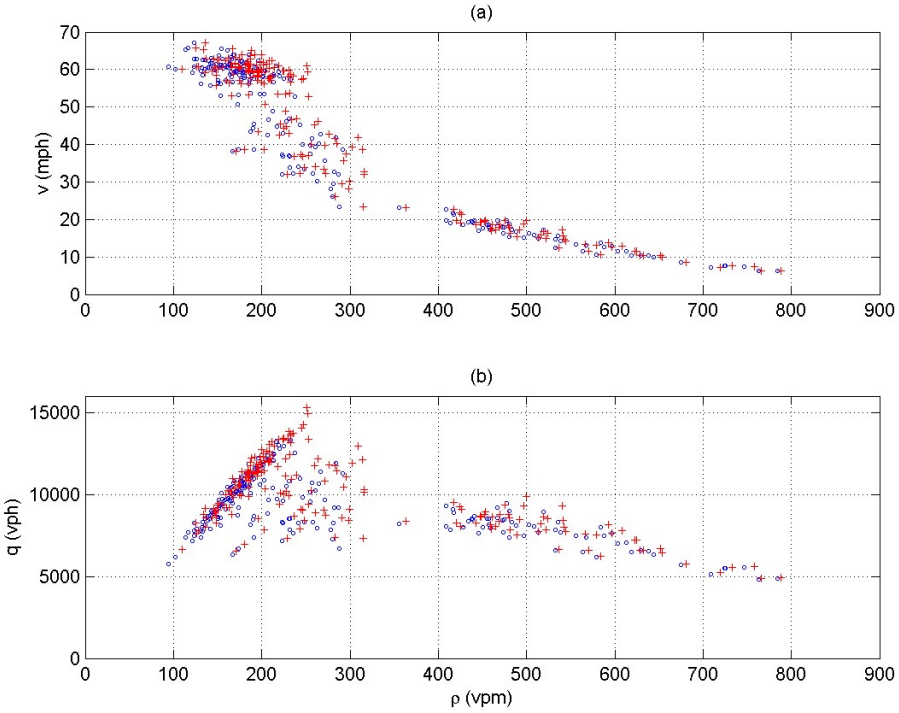

Figure 6: Fundamental diagrams with T=12, 35, 48, 56 s

with R-square 0.8040. From Figure 10, we can see that $q = \rho V(\rho)$ has a capacity of 13807 mph when $\rho = 249$ vpm, and $q = \rho V((1+\epsilon)\rho)$ has a capacity of 12709 mph when $\rho = 229$ vpm. The lane-changes cause a capacity drop of 7.95%.

The results indicate that lane-changing traffic is more active in $[950, 1400]$ than in $[1400, 1850]$. This is as expected, since the former section is immediately downstream to the on-ramp, while the latter is about 500 ft from the on-ramp and 510 ft from the off-ramp.

5.3 Different locations

In this subsection, we consider a road section $[500, 950]$, which is upstream to the on-ramp in Figure 1. From Figure 11, we find a linear relationship between density and lane-changing angle

$$\theta \quad = \quad -0.5921 + 0.0119\rho,$$

with R-square 0.8624. We can also find the following relationship between density and ϵ

$$\epsilon \quad = \quad 0.2570e^{-0.0046\rho},$$

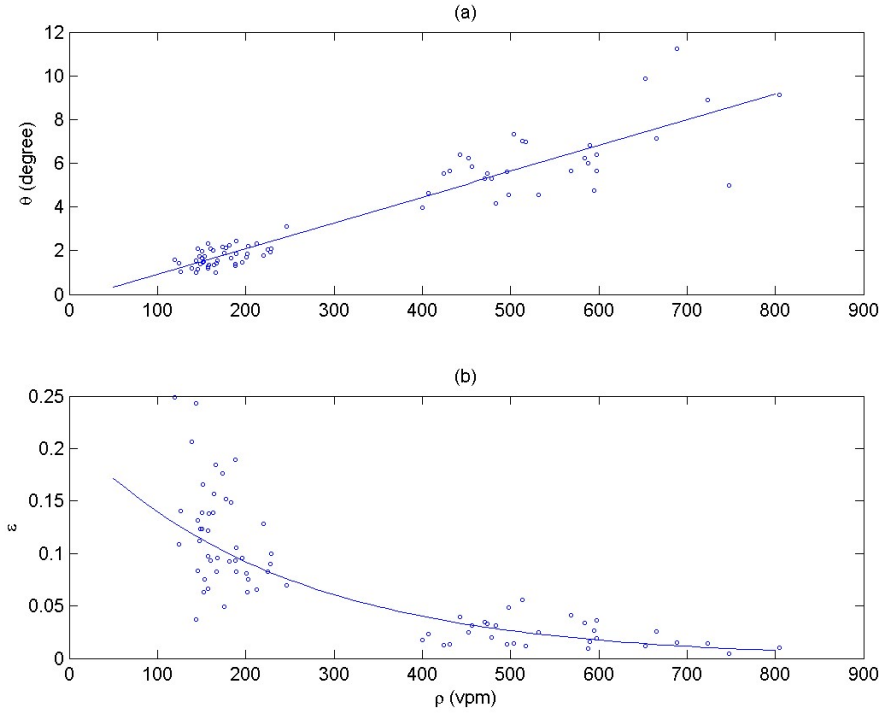

Figure 7: Characteristics of lane-changes for a road section $[950, 1400]$

with R-square 0.8561. From Figure 12, we can see that $q = \rho V(\rho)$ has a capacity of 13853 mph when $\rho = 251$ vpm, and $q = \rho V((1+\epsilon)\rho)$ has a capacity of 12301 mph when $\rho = 223$ vpm. The lane-changes cause a capacity drop of 11.20%.

Consistent with those in the preceding subsection, the results indicate that the lane-changing activity is more active in the upstream road section than in the downstream sections.

6 Conclusion

In this paper, we proposed a new interpretation of lane-changing intensity by following Edie's definition of traffic density and extended a macroscopic model of lane-changing traffic flow in our previous study. We also presented careful examinations of 75 minutes of vehicle trajectories collected for a freeway section on interstate 80. From the study, we found about 10% misidentified lane-changes caused by long shadows of vehicles at the boundaries of cameras. For different time intervals, cell sizes, and locations, we further verified the well-definedness of the lane-changing intensity variable and intensity-density relation. In addition,

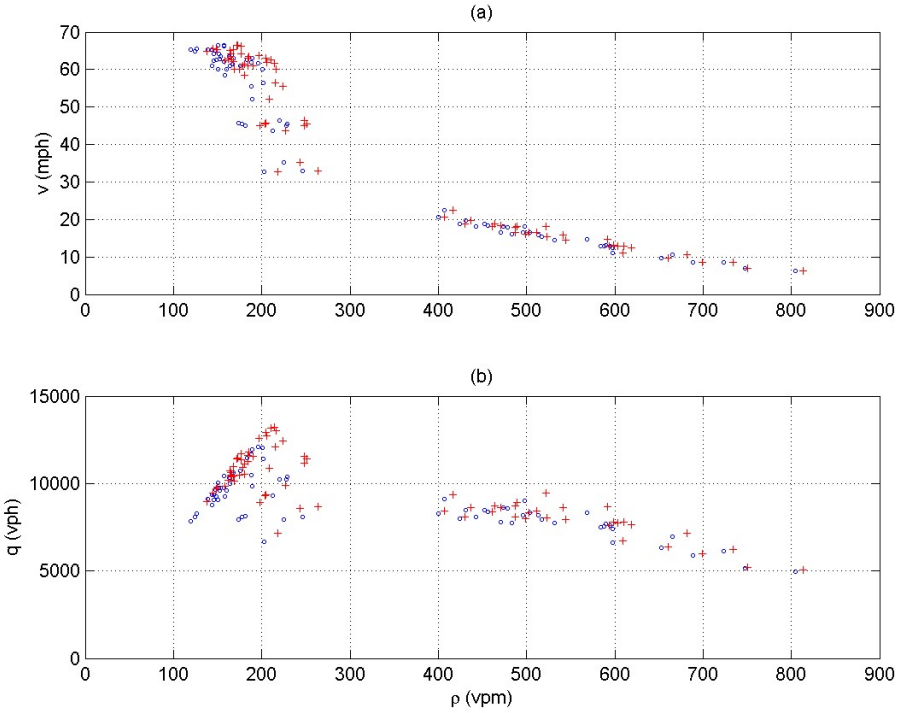

Figure 8: Fundamental diagrams for a road section $[950, 1400]$

the lane-changing angles are highly related to traffic density. Furthermore, we find that lane-changes can have significant impacts on the capacity of a multi-lane road. The observations demonstrate that the new theory can effectively capture the impacts of lane-changing traffic on overall traffic flow without looking into detailed lane-changing mechanisms.

This study is only the first attempt for us to understand macroscopic characteristics of lane-changing traffic, and many questions remain to be answered. With the new definition of lane-changing intensity in **Equation** 9, we will be able to study lane-changing intensity in other types of space-time domains, e.g., along vehicles' trajectories or shock waves. In the future, we will be interested in the impacts of on- and off-ramp traffic on lane-changing intensities. We will also be interested in determining a reasonable lane-changing threshold. One approach would be to compare capacities of a road section with and without lane-changes. But in the available I-80 data sets, lane-changing activities are quite consistent, and we will have to use other locations for this task. Furthermore, this new macroscopic model of lane-changing traffic is an approximation in nature and cannot describe many higher-order characteristics, e.g., capacity-drops caused by lane-changing. The new lane-changing intensity variable and intensity-density relation have to be verified with other observations in the future. Also we will be interested in studying individual vehicles' lane-changing times

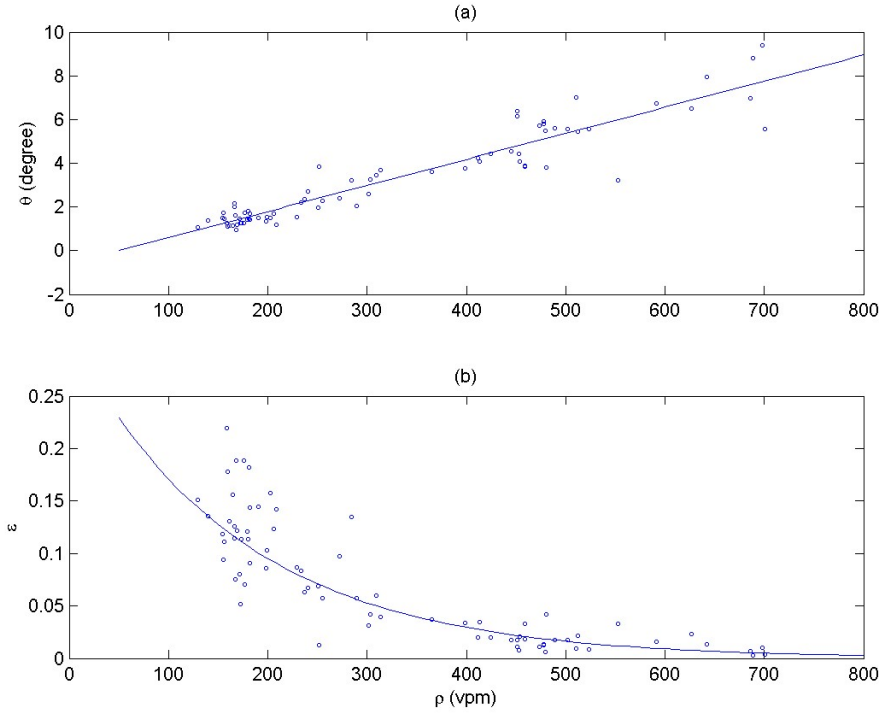

Figure 9: Characteristics of lane-changes for a road section $[1400, 1850]$

in different densities. Such studies could shed light on microscopic models of lane-changing traffic.

Acknowledgements

We would like to thank Dr. Shin-Ting (Cindy) Jeng and several anonymous reviewers for their valuable comments and discussions. The views and results herein are the author's alone.

References

[1] Fred L. Hall and Kwaku Agyemang-Duah. Freeway capacity drop and the definition of capacity. *Transportation Research Record: Journal of the Transportation Research Board*, 1320:91–98, 1991.

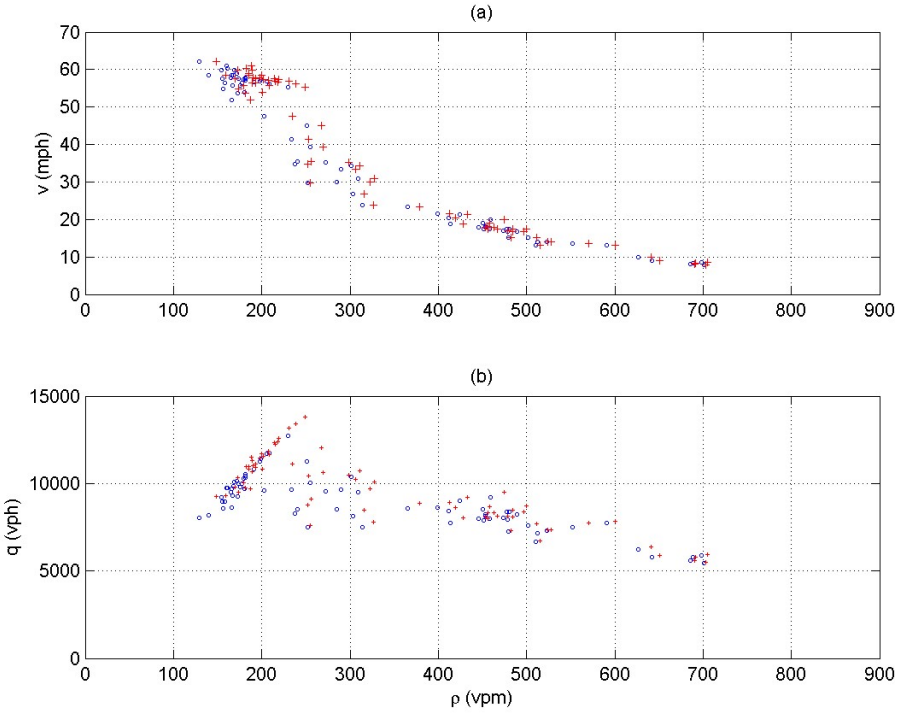

Figure 10: Fundamental diagrams for a road section $[1400, 1850]$

[2] Thomas F. Golob, Wilfred W. Recker, and Veronica M. Alvarez. Safety aspects of freeway weaving sections. *Transportation Research Part A*, 38(1):35–51, January 2004.

[3] P. G. Gipps. A model for the structure of lane changing decisions. *Transportation Research Part B*, 20(5):403–414, 1986.

[4] Qi Yang. *A Simulation Laboratory for Evaluation of Dynamic Traffic Management Systems*. PhD thesis, Massachusetts Institute of Technology, Cambridge, Massachusetts, 1997.

[5] Tomer Toledo, H. N. Koutsopoulos, and M. E. Ben-Akiva. Modeling integrated lane-changing behavior. In *Proceedings of Transportation Research Board Annual Meeting*, 2003.

[6] A. Kesting, M. Treiber, and D. Helbing. General Lane-Changing Model MOBIL for Car-Following Models. *Transportation Research Record: Journal of the Transportation Research Board*, 1999:86–94, 2007.

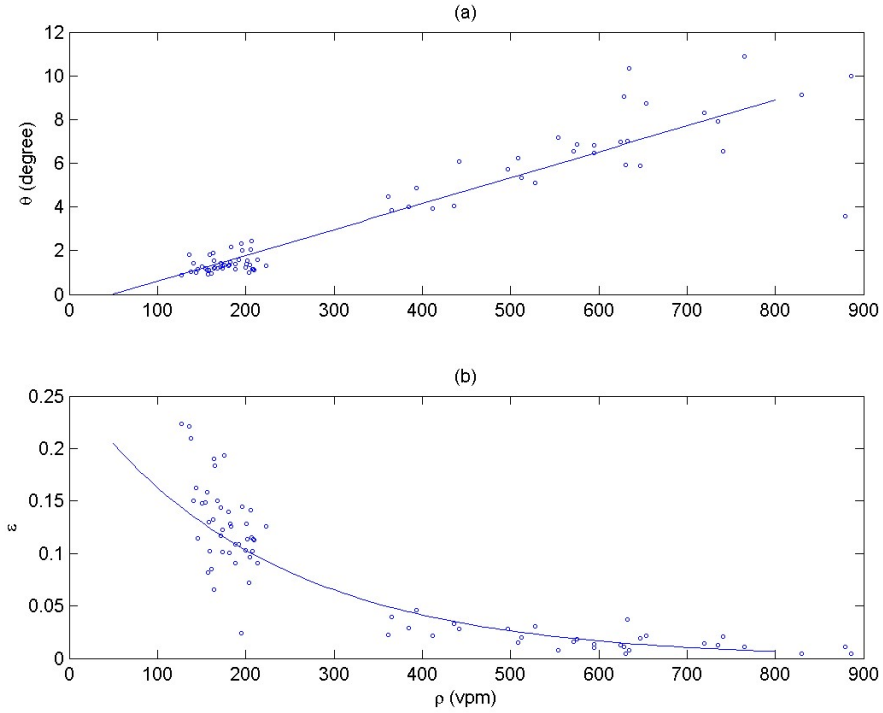

Figure 11: Characteristics of lane-changes for a road section $[500, 950]$

[7] PANOS G. Michalopoulos, DIMITRIOS E. Beskos, and YASUJI Yamauchi. Multilane traffic flow dynamics: Some macroscopic considerations. *Transportation Research Part B*, 18(4/5):377–395, 1984.

[8] Edward N. Holland and Andrew W. Woods. A continuum model for the dispersion of traffic on two-lane roads. *Transportation Research Part B*, 31(6):473–485, November 1997.

[9] Carlos F. Daganzo. A behavioral theory of multi-lane traffic flow. Part I: Long homogeneous freeway sections. II: Merges and the onset of congestion. *Transportation Research Part B*, 36(2):131–169, 2002.

[10] Benjamin Coifman. Estimating density and lane inflow on a freeway segment. *Transportation Research Part A*, 37(8):689–701, 2003.

[11] Denos C. Gazis, Robert Herman, and George H. Weiss. Density oscillations between lanes of a multilane highway. *Operations Research*, 10(5):658–667, 1962.

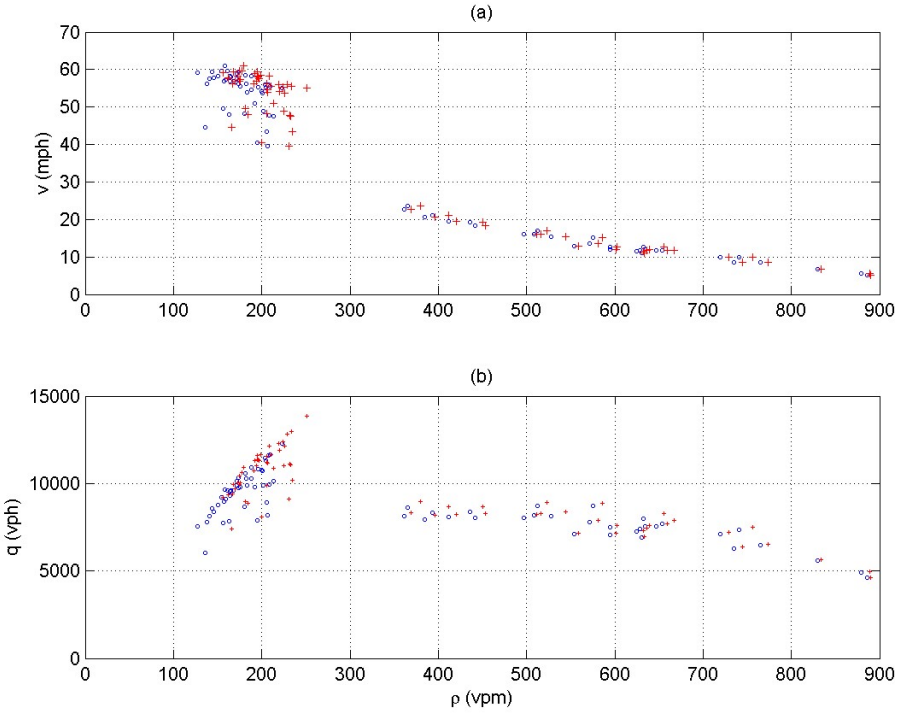

Figure 12: Fundamental diagrams for a road section $[500, 950]$

[12] P. K. Munjal and L. A. Pipes. Propagation of on-ramp density waves on uniform unidirectional multilane freeways. *Transportation Research*, 5:241–255, 1971.

[13] Wen-Long Jin, Yu Zhang, and Lianyu Chu. Measuring first-in-first-out violation among vehicles. In *Proceedings of Transportation Research Board Annual Meeting*, 2006.

[14] Jack E. Leisch. A new technique for design and analysis of weaving sections on freeways. *ITE Journal*, 49(3):26–29, 1979.

[15] J.A. Laval and C.F. Daganzo. Lane-changing in traffic streams. *Transportation Research Part B*, 40(3):251–264, 2006.

[16] W.-L. Jin. A kinematic wave theory of lane-changing traffic flow. *Transportation Research Part B*, 2010.

[17] B. D. Greenshields. A study in highway capacity. *Highway Research Board Proceedings*, 14:448–477, 1935.

[18] M. J. Lighthill and G. B. Whitham. On kinematic waves: II. A theory of traffic flow on long crowded roads. *Proceedings of the Royal Society of London A*, 229(1178):317–345, 1955.

[19] P. I. Richards. Shock waves on the highway. *Operations Research*, 4(1):42–51, 1956.

[20] LC Edie. Discussion on traffic stream measurements and definitions. In *Proceedings*, page 139. Organisation for Economic Co-operation and Development, 1965.

[21] M.J. Cassidy and B. Coifman. Relation among average speed, flow, and density and analogous relation between density and occupancy. *Transportation Research Record: Journal of the Transportation Research Board*, 1591:1–6, 1997.

[22] Federal Highway Administration. Next Generation SIMulation Fact Sheet. Technical report, December 2006. FHWA-HRT-06-135.

[23] Cambridge Systematics, Inc. NGSIM BHL Data Analysis. Technical report, September 2004. Summary Report, Prepared for Federal Highway Administration.

[24] Cambridge Systematics, Inc. NGSIM I-80 Data Analysis (4:00 p.m. to 4:15 p.m.). Technical report, September 2005. Summary Report, Prepared for Federal Highway Administration.

[25] Cambridge Systematics, Inc. NGSIM I-80 Data Analysis (5:00 p.m. to 5:15 p.m.). Technical report, September 2005. Summary Report, Prepared for Federal Highway Administration.

[26] Cambridge Systematics, Inc. NGSIM I-80 Data Analysis (5:15 p.m. to 5:30 p.m.). Technical report, September 2005. Summary Report, Prepared for Federal Highway Administration.